Eur. J. Mineral.
2004, **16**, 469–482

White micas with mixed interlayer occupancy: a possible cause of pitfalls in applying illite Kübler index (“crystallinity”) for the determination of metamorphic grade

PÉTER ÁRKAI[1]*, KENNETH J. T. LIVI[2], MARTIN FREY[3†], ALICE BRUKNER-WEIN[4] and CSANÁD SAJGÓ[1]

[1]Laboratory for Geochemical Research, Hungarian Academy of Sciences, Budaörsi út 45, H-1112 Budapest, Hungary
*Corresponding author, e-mail: arkai@geochem.hu
[2]Department of Earth and Planetary Sciences, Johns Hopkins University, Baltimore, Maryland 21218, USA
[3]Mineralogisch-Petrographisches Institut der Universität, Bernoullistrasse 30, CH-4056 Basel, Switzerland,
[†]deceased on the 10th of September, 2000
[4]Geological Institute of Hungary, Stefánia út 14, H-1143 Budapest, Hungary

Abstract: Integrated microstructural observations, X-ray powder diffractometric (XRPD) modal composition, illite Kübler index and chlorite “crystallinity” determinations and vitrinite reflectance measurements were carried out on marly slates from selected profiles of the Helvetic zone of the Central Alps, Switzerland. The studied profiles were: Upper Jurassic from the Wildhorn nappe, Brienz, Upper Jurassic from the Parautochthonous of the Aar massif, Glarus Alps, Eocene from the Griesstock nappe of the Glarus Alps and Upper Jurassic from the Axen nappe, Rhine Valley. In some of the localities studied, illite Kübler index (“crystallinity”) values were anomalously high, yielding only diagenetic conditions, while chlorite “crystallinity” and vitrinite reflectance showed anchi- and epizonal metamorphic conditions. Detailed XRPD observations carried out on Ca-saturated and glycolated mounts indicated subordinate amounts of swelling (smectitic) interstratifications in white mica. In addition to the dominant K-white mica, traces of discrete paragonite and paragonitic phases and tobelitic impurities in the form of either regular interstratifications or micas with mixed ($K>>Na>NH_4$) interlayer compositions could be detected from the XRPD (00,10) basal reflections. On the basis of the organic maturity assumed from vitrinite reflectance, probable partitioning of N and H between organic and inorganic phases, and the results of elemental (C, H, N, S) analyses carried out on the <2 μm fraction decarbonated and oxidized samples, the amount of NH_4^+ fixed in inorganic phases could be estimated. Small, but systematically appearing, absorption bands between 1400 and 1440 cm^{-1} in the FTIR spectra unequivocally proved the presence of ammonium in the rocks studied. Small amounts of N within the mica flakes were detected by electron energy loss spectrometry (EELS), confirming that NH_4^+ is indeed fixed in the interlayer site position. Energy dispersive spectroscopy (EDS) using scanning transmission electron microscopy (STEM) revealed heterogeneities in the interlayer cation occupancies. Although K is always dominant, irregular, local, domain-like enrichments in Na could be seen. The most accurate model to describe the disequilibrium state of the incipient metamorphic white micas studied is that of a dioctahedral mica structure with irregularly varying interlayer occupancies combined with subordinate amounts of swelling mixed-layers. The present work shows that, if these white micas are to be used for metamorphic petrogenetic purposes, special attention should be paid to their detailed characterization, especially in organic matter rich lithologies often characterized by high Al/Si bulk chemical ratios. Seemingly, white micas with mixed interlayer occupancies may be more widespread than has generally been anticipated so far.

Key-words: dioctahedral white micas, interlayer occupancy, chlorite, “crystallinity”, very low-grade metamorphism.

Introduction

The Kübler index (illite “crystallinity”) (abbreviated as KI) (Kübler, 1967, 1990) has been accepted and applied worldwide as a diagnostic tool for determining diagenetic and incipient metamorphic grades of clastic sedimentary sequences (for recent reviews see Merriman & Peacor, 1999; Árkai, 2002). The KI values represent the calibrated full width at half maximum (FWHM) of the first 10 Å basal reflections in X-ray powder diffraction (XRPD) data of dioctahedral K-white mica (measured on the <2 μm spherical diameter equivalent (SED) grain-size fraction).

Temperature has been regarded as the most important factor affecting the KI. As a rule, KI decreases (*i.e.*, “crystallinity” increases) with increasing temperature (~burial). The change in the KI value is attributed to: 1) a decrease in the proportion of swelling (smectitic) mixed-layers (especially at low-temperature diagenetic conditions), 2) an increase of the mean thickness of crystallites, often caused by a decrease in the amount of defects (usually planar) affect-

0935-1221/04/0016-0469 $ 6.30
DOI: 10.1127/0935-1221/2004/0016-0469

ing the coherency of layer-to-layer bonding (*i.e.*, an increase in the size of crystallites or domains that coherently scatter X-rays), and 3) a decrease of lattice strain (distortions) of crystallites. These changes are generally accompanied by changes in mineral chemistry – the most dramatic being the increase of layer charge and interlayer cation content. The KI method (often combined with other techniques such as vitrinite reflectance (R) measurements, determination of conodont colour alteration index (CAI), stable O and C isotope measurements, *etc.*) has proved to be a useful empirical tool for deciphering metamorphic (tectono-thermal) histories of basinal and folded thrust belt regimes (see the review of Merriman & Frey, 1999).

However, the anomalous behavior of illite-dioctahedral white mica as compared to other grade indicators has been reported often and was summarized by Frey (1987). An advanced illite "crystallinity" relative to other grade-indicating parameters can be found in sequences strongly affected by inherited (detrital) white mica or those characterized by high porosity and permeability which enhance the circulation of K-containing fluids. In contrast, retarded "crystallinity" KI values are frequently observed in cases when the reaction progress of illite-muscovite is hindered by physical and/or chemical conditions such as low permeability and porosity, considerable amounts of finely dispersed carbonate minerals and/or organic matter isolating the phyllosilicate grains, deficiency of K in the pore fluids, and high confining and H_2O pressures acting against the devolatilization process of the smectitic intercalations. Using the experience of many authors, Frey (1987) stated that the presence of other phyllosilicates with near 10 Å basal reflections may cause a broadening of the illite 10 Å peak. Such minerals are: pyrophyllite, paragonite, margarite, biotite and mixed-layer paragonite/muscovite.

The aim of the present paper is to elucidate an additional factor affecting KI that has not been considered so far – namely the presence of the ammonium cation in the interlayer position of the illite-white mica structure, and to evaluate its role in reaction progress of illitic material. The studied material derives from various parts of the Helvetic zone of the Swiss Central Alps.

Previous data on the role of NH_4^+ in the structure, mineral chemistry, and genesis of illite-dioctahedral white mica

Early reports on ammonium substituting for potassium in interlayer position of white mica structure have been published by Stevenson & Dhariwal (1959) and Vedder (1965). NH_4^+-bearing 'sericite' has been described by Yamamoto & Nakahira (1966), Yamamoto (1967) and Kozáč *et al.* (1977). NH_4^+-bearing micas, illite and illite/smecitite interstratified clay minerals were also hydrothermally synthesized (Barrer & Denny, 1961; Barrer & Dicks, 1966; Eugster & Munoz, 1966; Levinson & Day, 1968; Wright *et al.*, 1972; Tsunashima *et al.*, 1975; Shigorova *et al.*, 1981, Voncken *et al.*, 1987 and Šucha *et al.*, 1998).

In general, NH_4^+-bearing dioctahedral white micas and their precursor phases (NH_4^+-bearing illite/smectite interstratified clay minerals and NH_4^+-bearing illite) have been described predominantly from three different geological settings: 1) hydrothermal deposits including hydrothermally altered black shales, 2) organic matter-rich, diagenetically altered black shales and their very low-grade metamorphic equivalents, and less commonly, 3) NH_4^+-bearing muscovites from higher-grade metamorphic rocks.

Higashi (1978) described NH_4^+-dominant dioctahedral mica minerals, determined their chemistry and structural parameters, and called them tobelite (NH_4^+-bearing illite) after the hydrothermal pyrophyllite deposit of Tobe mine, Japan (Higashi, 1982). Yamamoto & Nakahira (1966), Kozáč *et al.* (1977), Šucha *et al.* (1993) and Bobos & Ghergari (1999) described ammonium-bearing illites with moderate swelling characteristics (minor smectitic interstratifications) from hydrothermally altered andesitic rocks. Sterne *et al.* (1982) described ammonium-bearing illites with 1.44–1.48 weight % NH_4^+ from hydrothermally altered black shales hosting a stratiform base metal deposit. Hydrothermal tobelitic veins were found in black shales by Wilson *et al.* (1992). In the latter two cases, introduction of NH_4^+ by hydrothermal fluids was proposed. The thermal degradation of organic matter might serve as an additional factor.

On the other hand, NH_4^+, released from dispersed organic matter maturing during diagenesis and very low-grade metamorphism, may be incorporated into silicate (particularly phyllosilicate) structures (Stevenson & Dhariwal, 1959; Hallam & Eugster, 1976, *etc.*). Duit *et al.* (1986) found that the NH_4^+ concentrations in muscovite and biotite decrease with increasing temperature. They found *ca.* 500 g/t NH_4^+ at the biotite isograd and *ca.* 120 g/t at conditions of anatexis in muscovite. Considering a possible solvus relationship between tobelite and muscovite, NH_4^+ in K-white micas has been investigated for potential thermometric uses (Guidotti & Sassi, 1998). According to these authors, high pressures would favor an increase in the NH_4^+ content in muscovite because an increase in phengite content in high-P muscovite causes a concomitant increase of size of the interlayer (XII) site. This makes the interlayer site more appropriate for the larger NH_4^+ ion.

In subgreenschist facies conditions, NH_4^+-bearing white micas occur over the whole temperature range. Juster *et al.* (1987) described NH_4^+-bearing illite from very low-grade mudrocks associated with anthracite and semi-anthracite coal ranks (T = *ca.* 200–275°C). These authors suggested that the ammonia was derived from the thermal decomposition of organic matter prior to complete graphitization of the carbonaceous material. Similar conclusions were made for clay mineral authigenesis in coals and shales by Daniels & Altaner (1990), Šucha *et al.* (1994), Ward & Christie (1994), Liu *et al.* (1996), *etc.*

The fixation of NH_4^+ by wetting and drying (*i.e.*, formation of NH_4^+-bearing illitic interstratifications during sedimentation and early diagenesis) was experimentally modeled by Šucha & Širáňová (1991). Cooper & Abedin (1981) determined considerable amounts of fixed interlayer NH_4^+ in the Gulf Coast shales. The genetic relations between diagenetic maturation of organic matter and ammonium substitution in illite were outlined by Williams *et al.* (1989), Williams & Ferrel (1991), Compton *et al.* (1992) and Schroeder

Tab. 1. List and characterization of selected samples investigated.

sample No. (MFAP-)	locality	rock type	stratigraphic age	formation	tectonic unit	Swiss coordinates	altitude (a.s.l., m)
4	Brienz-E, locality Balm at Ballenberg	limy marl	Jurassic (Bathonian – Oxfordian)	Erzegg Series	Wildhorn nappe, Helveticum	647.650/177.250	~730
36, 37, 39	Klausenpass road, W of the pass, overthrusted Cretaceous and Tertary slices (Glarus Alps)	silty, marly slate	Tertiary (Eocene: Lutetian to) Priabonian)	"Globigerina shales"	Griesstock nappe, Helveticum	704.400/192.100	~1600
41	Calfeisental, northern side, W of village Vättis, E of Gigerwaldsee (Glarus Alps)	marly slate	Upper Jurassic	"Schilt-schichten"	Parautochthonous of the Aar Massif, Helveticum	750.475/197.900	~1240
61, 65i, 65im, 67	Fläscherberg, western flank, "Mozentobel" (Rhine Valley)	marly slate	Upper Jurassic	Quinten limestone	Axen nappe Helveticum	755.700/212.450	~640

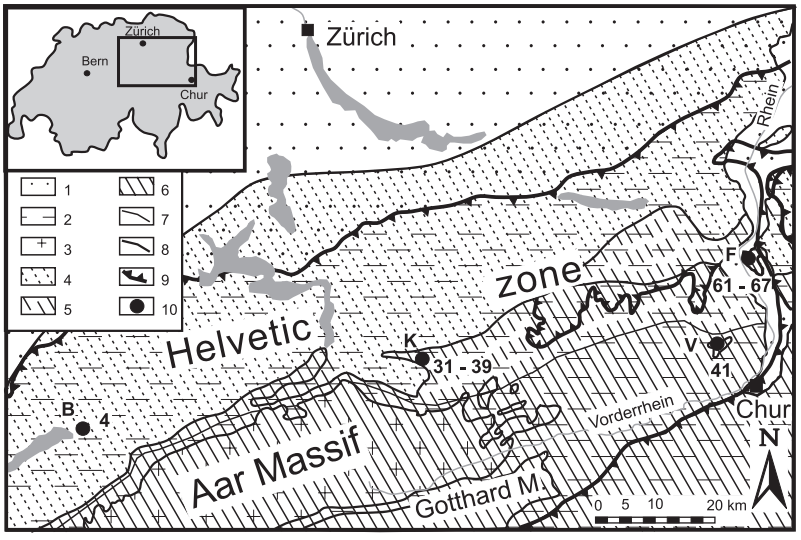

Fig. 1. Metamorphic map of the Helvetic zone, Swiss Central Alps, strongly simplified after Frey *et al.* (1999), with the localities studied. Legend: 1 – Alpine molasse, Quaternary deposits; 2 – cover units (Late Carboniferous – Cretaceous or Eocene); 3 – basement units: Variscan granitoids (not-metamorphosed during pre-Alpine times) and sedimentary rocks and metasediments (pre-Alpine partly not metamorphic, partly greenschist facies); 4 – folded, non-metamorphic; 5 – very low-grade metamorphic (~anchizone); 6 – low-grade metamorphic (~epizone); 5 and 6: Tertiary peak metamorphism; 7 – boundary between metamorphic grades; 8 – boundary of main units; 9 – main overthrust plain; 10 – sampling locality. Abbreviations: B – village Brienz-East, locality Balm at Ballenberg; K – Klausenpass road, west of the pass; V – west of village Vättis, northern side of the Calfeisental; F – Fläscherberg, western flank: "Mozentobel".

& McLain (1998). They have found that fixed NH_4^+ increased with the proportion of authigenic illite formed from illite/smectite. The maximum fixation of NH_4^+ per unit of authigenic illite occurred within the 'oil window' characterized by rapid thermal breakdown of organic matter that released NH_3 or NH_4OH. Consequently, NH_4^+ fixed in illite may serve as an indicator of organic maturity and hydrocarbon migration pathways. Drits *et al.* (1997) and Sakharov *et al.* (1999) elaborated XRPD profile fitting methods for determining the content and distribution of fixed ammonium in illite/smectite. They proved that illite/smectites from the North Sea Upper Jurassic contained K end-member illite and NH_4^+ end-member tobelite layers – the latter being characteristic of diagenesis and oil generation.

Depending on the nature of the illite/smectite starting material in Upper Jurassic and Cambrian black (alum) shales, the mechanisms of diagenetic/anchimetamorphic tobelitization may be different. However, they are always linked to oil generation that liberates ammonium from the organic matter (Lindgreen *et al.*, 2000). On the basis of genetic (temporal, spatial, chemical and physical) interrelations between the NH_3 release from kerogen during maximum oil generation and fixation of NH_4^+ in tobelite layers in illite/smectite, Drits *et al.* (2002) proposed the 'tobelitization window' which may be present in all oil-source rock shales. The 'tobelitization window' is characterized by random vitrinite reflectance range of R_{random} = 0.6–0.7% that roughly corresponds to a temperature range of 100–140°C. In this range, the three-component illite/smectite/vermiculite interstratified clay mineral transforms into the four-component illite/tobelite/smectite/vermiculite mineral.

Using great variety of electron microbeam, XRPD, FTIR and chemical methods, Nieto (2002) demonstrated that NH_4^+ and K^+ are present in the same interlayer of dioctahedral white mica, with one of them being dominant. Tobelitic and muscovitic micas form distinct packets in the very low-grade metapelites. Intergrowth of the packets are rare and interstratification is practically lacking.

Study samples

The samples studied in the present paper derive from four localities of the outer thrust and fold belt of the Swiss Cen-

tral Alps, namely from the Helvetic zone (Fig. 1). These materials were selected from a large sample group containing 70 samples, collected by two of the authors (MF and PÁ) in 1997 for studying eventual relations between phyllosilicate crystallinity and tectonic strain. Their lithologies are rather similar including marls and marly, silty slates alternating with limestones. The samples represent various formations from different nappe or parautochthonous units of the Helvetic zone (Table 1). Their sedimentary ages vary from Middle Jurassic to Late Eocene. According to the new "Metamorphic Maps of the Alps" (Frey *et al.*, 1999) and references therein, the rocks at the Brienz locality (B in Fig. 1) are only diagenetically altered, while those from Klausenpass (K) and Fläscherberg (F) experienced very low-grade (anchizonal), and those of Vättis (V) reached low-grade (epizonal) regional metamorphic conditions peaking during the Tertiary.

Methods

Conventional petrographic meso- and microscopic observations were aimed at the determination of rock types and their microstructural features, with a special reference to the discrimination of detrital (inherited) and newly formed (diagenetic and metamorphic) minerals. The XRPD work was carried out in the laboratory for Geochemical Research, Budapest. XRPD patterns were obtained from both non-oriented and highly-oriented powder mounts of whole rock samples and their <2 μm spherical equivalent diameter (SED) size fractions, using a Philips PW-1730 diffractometer with computerized APD system. Air-dried (AD), Ca-saturated (with 0.5 mol l^{-1} $CaCl_2$ solution) and air-dried (Ca,AD), and glycolated (EG and Ca,EG) mounts were obtained and studied. The procedures of sample preparation and treatments, as well as the XRPD instrumental and measuring conditions and their errors, were described in detail by Árkai *et al.* (2002).

XRPD data were used for the determination of modal composition and values of KI and chlorite "crystallinity" (ChC, the FWHM values of the first (14 Å) and second (7 Å) basal reflections of chlorite, denoted as ChC(001) and ChC(002), respectively). The semi quantitative modal composition of the whole rock and <2 μm fraction samples was calculated by the direct method of Bárdossy (1966) and Bárdossy *et al.* (1980), with the addition of bulk rock major element chemical compositions and DTG data. (For the errors and uncertainties of this procedure, see Bárdossy *et al.*, 2001.) The calibration of illite "crystallinity" and ChC values to Kübler's KI scale was made using standard rock slab series (Nos. 32, 34 and 35) provided by B. Kübler, and a least-squares method was used so that the KI boundaries of the anchizone corresponded exactly to 0.25 and 0.42°Δ2Θ. Consequently, the anchizone boundaries of ChC(001) and ChC(002) in the present paper are 0.26–0.38 and 0.24–0.30°Δ2Θ for fine-clastic metasedimentary rocks (Árkai *et al.*, 1995). All of these boundary values refer to air-dried (AD) mounts. Apparent mean crystallite thickness and lattice strain of illite/K-white mica and chlorite were calculated from line-profiles of XRPD basal reflections by the Voigt method of Langford (1978) (as modified by the Philips APD-1700 software package) using the DECPROF PC program of A. Nagy written for the Laboratory for Geochemical Research, Budapest. (For the description of the calculation and its errors see Árkai *et al.*, 2002.)

Vitrinite reflectance (R_{random}, R_{max}, R_{min}) values of dispersed coalified particles were measured in the Lab. for Geochemical Research, Budapest, on grains with diameters equal or larger than 3 μm, as described by Árkai (1983). Elemental (N, C, H, S) analysis of the <2 μm fraction samples was performed on an NA 1500 NCS Analyser (Fisons Instruments, Inc., Beverly, MA) at 1020°C, in the Geological Institute of Hungary, Budapest. This analytical method is based on the complete and instantaneous oxidation of the sample by "flash combustion" which converts all organic and inorganic substances into combustion products. The gas products pass through a reduction furnace and go into the chromatographic column by the carrier gas (He). The products are detected by a thermal conductivity detector (TCD).

The IR spectra were recorded with a Perkin-Elmer 1600 Series spectrophotometer using the KBr technique in the Geological Institute of Hungary, Budapest. Infrared bands were assigned according to the data of Van der Marel & Beutelspacher (1976) and Farmer (1974). The removal of organic carbon content (dissolving the organic matter via oxidation) may affect the white mica and chlorite structures and compositions. In order to evaluate these effects, experiments on model samples were carried out. The samples were treated with H_2O_2, $KMnO_4$ and $K_2Cr_2O_7$ both in acidic and basic solutions (Table 2). Judging from the KI values measured on illite-muscovite and the ChC(001) and ChC(002) values of chlorite, only the H_2O_2 treatment (digested in a water-bath for 4–16 hours) did not significantly modify these phyllosilicates. Therefore, this method was chosen and applied until the samples turned to a white colour. In order to remove the remaining traces of inorganic carbon (carbonates), the <2 μm fraction samples were decarbonated with a 10% cold acetic acid and an additional HCl rinse. After oxidation and the repeated decarbonation, the IR spectra of samples were recorded as well.

Electron energy loss spectroscopy (EELS, see also Livi *et al.*, 2001) and scanning transmission electron microscopy (STEM) analyses were performed on selected samples at the Department of Earth and Planetary Sciences, Johns Hopkins

Tab. 2. Effects of chemical treatments used for oxidizing the dispersed organic matter on the illite Kübler index and chlorite "crystallinity" values measured on the <2 μm grain-size fraction samples, previously decarbonated by 10 % cold acetic acid.

sample No.	treatment	KI	ChC(001)	ChC(002)
MFAP-36	*not treated*	*0.585*	*0.284*	*0.248*
	H_2O_2	**0.571**	**0.298**	**0.238**
	$H_2SO_4 + K_2Cr_2O_7$	0.755	n.m.	n.m.
	$H_2SO_4 + H_2O_2$	0.723	n.m.	n.m.
	$NaOH + KMnO_4$	0.601	0.272	0.286
	$H_2SO_4 + KMnO_4$	0.577	n.m.	n.m.
	HNO_3	0.636	n.m.	n.m.

n.m. = not measurable beause reagents dissolved the chlorite phase
Values in Δ°2θ, CuK_α (for details see the part "Methods")

Tab. 3. Modal compositions determined by XRPD.

sample	whole rock								<2 µm fraction									
(MFAP-)	Qtz	Ab	10-Å*	Chl	Cal	Dol	Py	Rt	Qtz	Ab	Ill-Ms	I/S	I/Pg	Pg	I/T	Chl	Py	Rt	Goe
4	x		x	tr	+	o	tr		o		+	tr			?tr	o	o		
36	x	o	x	x	x		o		o		+	tr	tr	tr	?tr	x	tr		
37	x	o	x	x	x		o		o		x	tr	tr	tr	?tr	x		?tr	
39	x	o	x	x	x	o	tr		o		+			o	?tr	x	tr		
41	x	o	x	o	x	o	tr	?tr	o		+				?tr	o	tr	?o	
61	o		x	o	+	o	tr		tr		+	tr	tr	x	?tr	x			
65i	x		o	o	+	o	o		o		+	tr	tr	x	?tr	x	tr		tr
65im	x	o	o	x	+	o	o		o		+	tr	tr	x	?tr	x	tr		
67	o		x	x	+	o	o	?tr	o		+	tr	tr	x	?tr	o	tr		

Abbreviations after Kretz (1983), except 10-Å* = dioctahedral mica-like phyllosilicates, predominantly illite-muscovite; Ill-Ms = illite-muscovite; I/S = illite/smectite interstratified clay mineral; I/Pg = mixed (K>Na) white mica; I/T = mixed (K>NH_4-bearing white mica)-
Legend: + = dominant (*ca.* >50 %)
x = significant (*ca.* 10–50%)
o = subordinate (*ca.* 1–10 %)
tr = traces

University, Baltimore. The sample was prepared from whole rock chips by grinding in a mortar and pestle and ultrasonic dispersion in distilled water. A holey-carbon copper TEM grid was dipped into the mineral suspension and dried. This method produced large thin crystals ideal for EELS and STEM analysis. No further preparation was necessary. EEL spectra were generated using a Philips CM 300 FEG operating at 297 kV, 3 kV extraction voltage, and in the image mode with a magnification of 49 kX (semi-angle of divergence of 100 mrad). The EELS data were recorded from thin electron-transparent areas lying over holes in the support film. Selected area electron diffraction was obtained before and after analysis to observe the extent of beam damage. Energy dispersive X-ray STEM maps were obtained using an EmiSpec analyzer coupled with an Oxford instruments light element detector and XP3 pulse processor. Images were generated at approximately 70,000X with a defocused beam to reduce beam damage.

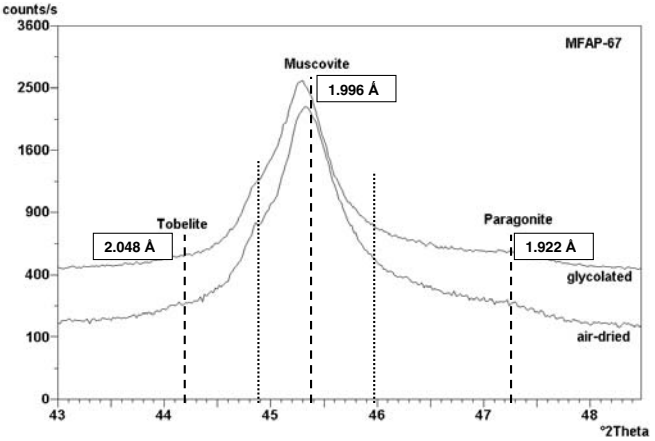

Fig. 2. Details of X-ray powder diffractograms of a <2 µm size fraction sample. Dashed lines correspond to the theoretical positions of the (00,10) reflections of tobelite, muscovite and paragonite, respectively. Dotted lines refer to the presence of mixed phases. For further details see the text.

Results and discussion

Modal composition and characterization of the dominant phase

Table 3 shows the modal compositions determined by XRPD of the selected samples. In the whole rock samples, calcite was a frequent, often dominant mineral constituent, while dolomite was mostly subordinate or absent. Quartz, dioctahedral mica-like minerals, and chlorite were the main non-carbonate phases. Small or trace amounts of pyrite indicated reduced conditions. Albite occurred only rarely and always in minor quantities.

In the <2 µm fractions, dioctahedral K-rich mica-like structures (referred to as illite-muscovite) predominate. Sample glycolation caused small but significant changes in the shape of the 10 Å basal reflection which indicated the presence of swelling (smectitic) interstratifications. However, the smectitic abundance was always less than illite-muscovite. The (00,10) reflection near 2 Å ($2M_1$ polytype) was used for determining the interlayer cation species. Fig. 2 shows details of XRPD profiles from a representative sample. Glycolation caused little effect on the position and shape of the peaks. As compared to the position of ideal muscovite (45.40°2Θ = 1.996 Å), the main illite-muscovite peak was shifted towards lower °2Θ (*i.e.*, higher d values). This shift, together with the "shoulder" between the positions of illite-muscovite and tobelite (00,10) basal reflections, may indicate the presence of regularly interstratified, non-swelling structures or to mica structures with mixed interlayer occupancies where potassium was partially replaced by other cations with larger radii. Small, rather diffuse reflections at around 47.29°2Θ (1.922 Å) indicated the presence of small amounts of discrete paragonite (Fig. 2). According to Frey & Niggli (1972), the exact position of the (00,10) reflection can be used to discriminate between paragonite and margarite, the latter having a smaller basal spac-

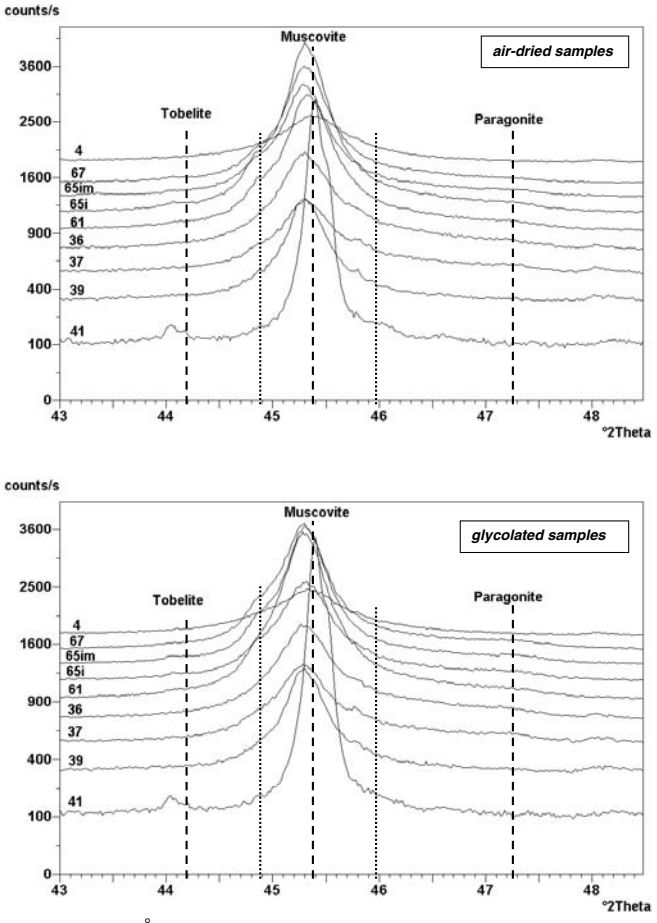

Fig. 3. Near 2 Å part of the diffractograms obtained from the <2 μm size fraction samples, showing the shift of the pattern from diagenetic (sample 4) to epizonal (sample 41) grade. For legend see the caption of Fig. 2.

ing (1.908 Å at 47.66°2Θ). Shoulder-like, diffuse peaks or an increase in the background between the illite-muscovite and paragonite reflections indicated that regularly interstratified Ms/Pg or mica with mixed (K>>Na) interlayer occupancy may be present. The XRPD data for the (00,10) reflections of samples ranging from diagenetic (sample 4) to epizonal grade (sample 41) are displayed in Fig. 3 for comparison.

In summary, the XRPD data revealed a diversity of dioctahedral mica-like structures present in the <2 μm grain-size fractions. K-rich, illite-muscovite with small amounts of swelling (smectitic) interstratifications predominated, but some interstratified and/or mixed K>>Na>NH_4(?) micas, accompanied by small amounts of discrete paragonite, were also present. However, the weak and rather uncertain XRPD signatures of the presence of NH_4-bearing mica needed further support from other methods. Similarly, further evidence was needed to clarify whether the micas with varying interlayer cation content represented mixed-layering or a domain structure.

In addition to dioctahedral white mica-like structures outlined above, considerable amounts of chlorite, lesser amounts of quartz, and traces of pyrite and rutile were also found in the <2 μm fractions.

XRPD-measured phyllosilicate "crystallinity"

Table 4 contains the calibrated KI and ChC values. For rough comparison, the 10 Å reflections of the Ca^{2+}-saturated and air-dried mounts are also displayed (Fig. 4). In accordance with the new metamorphic map of the Alps (Frey *et al.*, 1999), very large diagenetic KI values were obtained on the sample from locality Brienz (sample 4). In this sample, the relatively large difference (ca. 0.15°2Θ) between KI (Ca,AD) and KI (Ca,EG) (Table 4) indicated the presence of interstratified swelling components, the amount of which, however, was much less than that of illite.

In the anchizonal samples from the Klausenpass locality (K in Fig. 1, samples 36 to 39), KI strongly varied between diagenetic and anchizonal values in samples collected within a few tens of meters of each other. In these samples, Ca^{2+}-saturation and glycolation caused a rather small sharpening of the 10 Å reflection by 0.002–0.027°2Θ. This difference was considerably smaller than for sample 4 (0.15°2Θ). This indicated that there were smaller amounts of smectitic interstratifications in the Klausenpass samples than in the Brienz sample. Consequently, the strong variation in KI in the Klausenpass samples may be related to the incorporation of Na and possibly NH_4^+ into the K-dominated structures.

The samples from the Fläscherberg locality (F, samples 61 to 67) that underwent anchizonal metamorphism (Frey *et al.*, 1999) actually exhibited diagenetic KI values (Table 4).

Tab. 4. Illite Kübler index (KI) and chlorite "crystallinity" (ChC) indices obtained on the <2 μm grain-size fraction samples.

sample No. (MFAP-)	KI (AD)	KI (Ca^{2+},AD)	KI (Ca^{2+},EG)	ChC(001) (AD)	ChC(001) (Ca^{2+},AD)	ChC(001) (Ca^{2+},EG)	ChC(002) (AD)	ChC(002) (Ca^{2+},AD)	ChC(002) (Ca^{2+},EG)
4	0.909	0.874	0.726	n.m.	n.m.	n.m.	0.305	0.327	0.342
36	0.641	0.611	0.609	0.352	0.351	0.321	0.288	0.287	0.300
37	0.564	0.546	0.519	0.319	0.308	0.296	0.271	0.256	0.258
39	0.378	0.351	0.342	0.299	0.295	0.285	0.260	0.250	0.257
41	0.220	0.236	0.233	n.m.	n.m.	n.m.	0.241	0.241	0.242
61	0.552	0.612	0.517	0.233	0.285	0.296	0.250	0.277	0.277
65i	0.680	0.748	0.610	0.241	0.261	0.263	0.258	0.281	0.275
65im	0.566	0.521	0.489	0.241	0.279	0.275	0.251	0.266	0.266
67	0.548	0.610	0.535	0.224	0.266	0.271	0.232	0.272	0.282

Calibrated values in Δ°2θ, CuK_α (for details see the part "Methods")
n.m. – not measurable because of the small intensity of the 14-Å peak

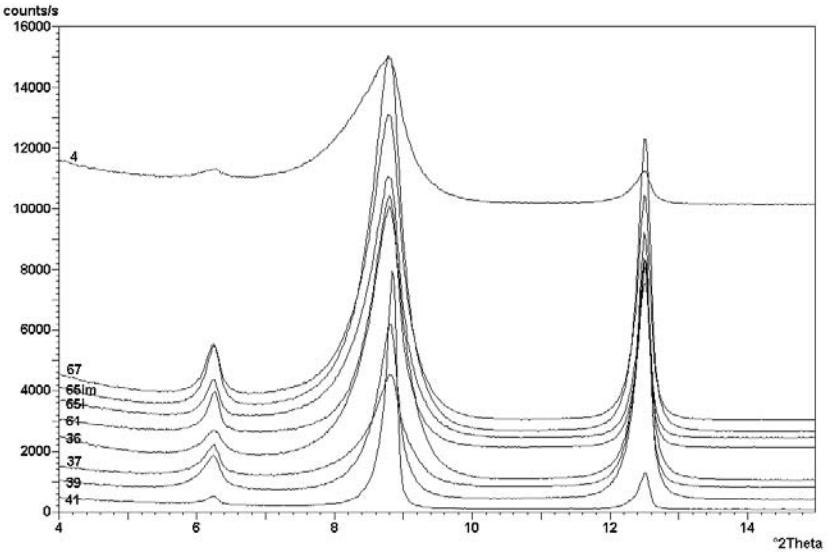

Fig. 4. Comparison of the shapes of the 10 Å XRPD reflections of the dioctahedral mica-like structures in the studied sample series that ranges from diagenetic KI zone (4) up to the epizone (41). Ca^{2+}-saturated and air-dried (Ca^{2+},AD) mounts.

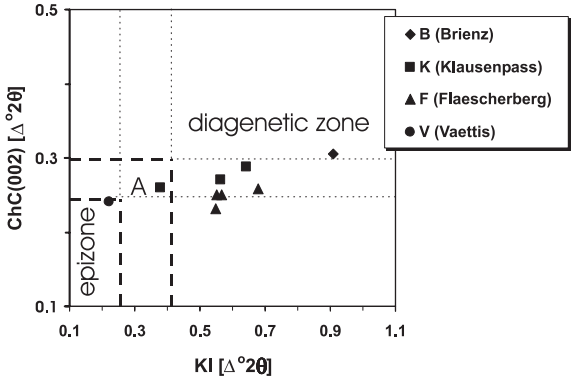

Fig. 5. Relation between illite Kübler index and chlorite "crystallinity" values obtained on air-dried mounts. The boundary values of the anchizone are after Kübler (1967, 1990) for KI and after Árkai *et al.* (1995) for ChC(002). A = anchizone.

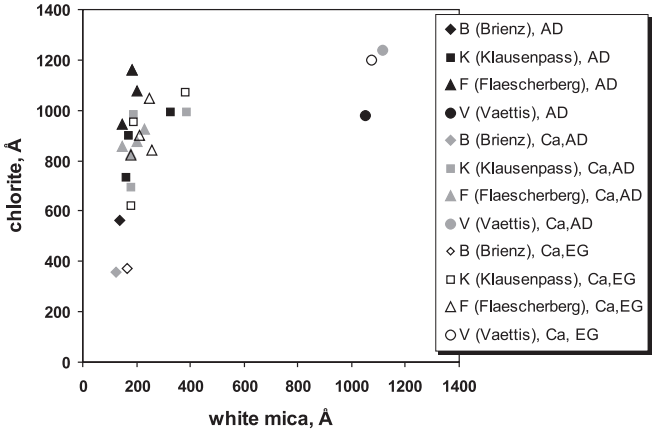

Fig. 6. Relationship between the apparent mean crystallite thickness values of dioctahedral white mica and chlorite determined from the 10 and 7 Å basal reflections, using the modified Voigt method. Black symbols: air-dried (AD), gray symbols: Ca-saturated and air-dried (Ca,AD); open symbols: Ca-saturated and glycolated (Ca,EG) mounts.

In most cases, Ca^{2+}-saturation caused small (0.060–0.068°2Θ) increases in the FWHM values of the 10 Å peak, while glycolation caused somewhat stronger decreases (0.032–0.138°2Θ). These changes may indicate the presence of small amounts of swelling (smectitic) interstratifications within illite-muscovite.

The sample from Vättis locality (V, sample 41) displayed epizonal KI values and agrees with earlier results summarized by Frey *et al.* (1999). In this sample, the illite-muscovite structure was "closed", *i.e.*, was unable to react to Ca^{2+}-saturation or glycolation.

As is shown by Fig. 5, the conclusions drawn from the diagenetic – metamorphic zones deduced from KI and ChC values were strongly conflicting. With reference to the chlorite "crystallinity" ranges previously determined for the anchizone (Árkai *et al.*, 1995), apparent contradictions were found between the calibrated KI and ChC values for most of the anchizonal Klausenpass (36–39) and Fläscherberg (61–67) samples. Indeed, in most cases, the ChC values showed anchizonal grade, in agreement with the new metamorphic map of Frey *et al.* (1999), whereas the KI data from the same samples were spread all over the KI range of the diagenetic zone. For example, ChC(002) values from Brienz (sample 4) were in the diagenetic range, ChC(001) and ChC(002) values from Klausenpass (samples 36 to 39) were of anchizonal grade, ChC(001) and ChC(002) values from the Fläscherberg locality (61 to 67) indicated partly anchi- and partly epizonal conditions, while ChC(002) values from Vättis (41) indicated transitional anchi-/epizonal conditions.

The above discrepancy between dioctahedral white micas and chlorites was also reflected in the apparent mean crystallite thicknesses of these minerals (Fig. 6). The majority of white micas exhibited diagenetic mean crystallite thicknesses, while only sample 39 had anchizonal and sample 41 epizonal values (for comparisons see Merriman & Peacor, 1999, and Árkai, 2002). Except for the epizonal sample, glycolation caused increases in mean thicknesses.

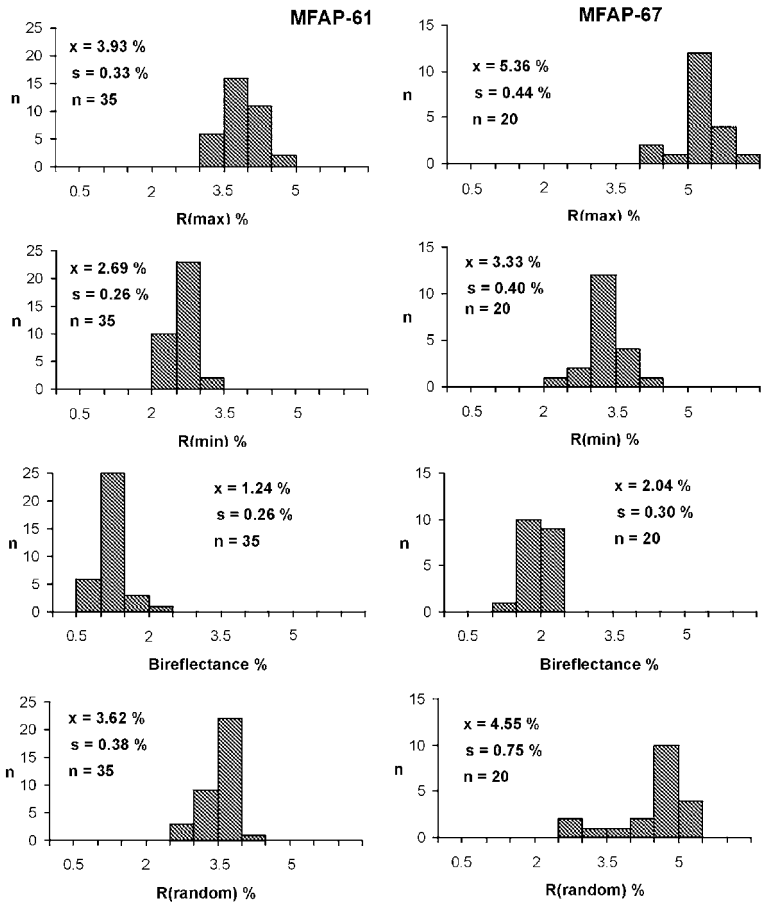

Fig. 7. Frequency distributions and statistical parameters of vitrinite reflectance data measured on marly slates from the Fläscherberg locality ("Mozentobel"), Eastern Switzerland.

The effects of Ca^{2+} saturation were much smaller and rather controversial. In contrast, chlorites displayed larger mean crystallite thicknesses than the white micas. The above apparent discrepancy will be clarified by additional data.

Vitrinite reflectance

Vitrinite reflectance (R) is another independent parameter for characterizing diagenetic and low-temperature metamorphic grades (for reviews see Kisch, 1983; Teichmüller, 1987; *etc.*). Vitrinite reflectance is useful in cases where the application of phyllosilicate "crystallinity" methods is hindered by the presence of more than one 2:1 phyllosilicate species or where there is considerable lattice strain.

Unfortunately, samples from Brienz (4) and Klausenpass (36-39) contained vitrinite grains and flakes too small (usually <1 μm in diameter) for proper reflectance measurements. The slates studied from Vättis (41) did not contain any coalified dispersed organic matter. The frequency distributions of the R data and their statistical parameters for the Fläscherberg samples are given in Fig. 7a (sample 61) and 7b (sample 67). The R_{random} and R_{max} averages unequivocally indicate anchizonal conditions with sample 67 being of high-anchizonal grade. The relatively large differences between the R values of the two Fläscherberg samples may be related to the contrasting meso-structural positions of the samples. Sample 61 was collected from the hinge of a tight recumbent outcrop-scale fold, while sample 67 was collected from the lower (inverted) limb of the same fold.

Unpublished R_{max} values of 7 samples from Fläscherberg range between 5.19 and 5.76% (Erdelbrock 1994, unpublished PhD thesis, Basel). One of the samples analyzed by Erdelbrock was located near our samples 61 and 67 and gave an R_{max} value of 5.24 ± 0.26%. This is similar to the value obtained by us for sample 67.

Consequently, both chlorite "crystallinity" and vitrinite reflectance data indicate anchizonal conditions at the Fläscherberg, "Mozentobel" locality and are in agreement with the new metamorphic map of the Alps. This is in contrast to the KI values which are too large – rendering them inappropriate for characterizing the metamorphic grade.

C, H, N and S elemental composition: measurements and estimates

The elemental compositions of the decarbonated as well as the decarbonated and oxidized <2 μm SED fraction samples are given in Table 5. The data were assumed to reflect both inorganic and organic phases. Sulfur concentrations of the decarbonated samples ranged from 0.7 to 0.06 weight % and may have been predominantly fixed by dispersed organic matter (S_{org}) and pyrite. The SO_4^{2-} form may also have been present, but in minor concentrations as indicated by the 0.0003–0.08 weight % concentrations of S in some oxidized samples.

Tab. 5. Elemental (C,H,N,S) analyses, probable partitioning of H and N between organic and inorganic phases and estimates of NH_4^+ and H_2O contents in the <2 μm grain-size, dioctahedral white mica-rich fraction samples.

sample No.	measured concentration in weight %							ratios		(atomic)	N_{inorg}	NH_4^+	*NH_4^+ (diff)*	H_{org}	H_{inorg}	H_2O
(MFAP-)	C	*C(diff)*	*H*	*H(diff)*	*N*	*N(diff)*	S	C/12	N/14	N/C	(wt%)[1]	(wt%)[2]	*(wt%)[2]*	(%)[3]	(%)[4]	(wt%)[5]
4	1.43		0.88		0.297		0.43	0.119	0.021	0.176	0.26	0.34		0.06	0.82	6.71
4 (oxidized)	*0.85*	*–0.58*	*0.82*	*–0.06*	*0.269*	*–0.028*	*0.08*	*0.071*	*0.019*	*0.268*	*0.25*	*0.32*	*–0.02*	*0.04*	*0.78*	*6.42*
36	1.21		0.80		0.190		0.16	0.101	0.013	0.129	0.16	0.21		0.05	0.75	6.33
36 (oxidized)	*0.74*	*–0.47*	*0.77*	*–0.03*	*0.235*	*0.045*	*0.00*	*0.062*	*0.017*	*0.274*	*0.22*	*0.28*	*0.07*	*0.03*	*0.72*	*6.09*
37	1.22		0.87		0.233		0.16	0.102	0.016	0.157	0.20	0.26		0.05	0.82	6.85
37 (oxidized)	*0.56*	*–0.66*	*0.76*	*–0.11*	*0.215*	*–0.018*	*0.00*	*0.047*	*0.015*	*0.319*	*0.20*	*0.26*	*0.00*	*0.02*	*0.74*	*6.11*
39	1.00		0.80		0.198		0.056	0.083	0.014	0.169	0.17	0.22		0.04	0.76	6.38
39 (oxidized)	*0.61*	*–0.39*	*0.85*	*0.05*	*0.269*	*0.071*	*0.0003*	*0.051*	*0.019*	*0.373*	*0.25*	*0.33*	*0.10*	*0.02*	*0.83*	*6.77*
41	1.65		0.79		0.211		0.12	0.138	0.015	0.109	0.17	0.22		0.07	0.72	6.05
41 (oxidized)	*0.49*	*–1.16*	*0.69*	*–0.10*	*0.163*	*–0.048*	*0.00*	*0.041*	*0.011*	*0.268*	*0.15*	*0.19*	*–0.03*	*0.02*	*0.67*	*5.64*
61	2.41		0.88		0.310		0.32	0.201	0.022	0.109	0.25	0.33		0.1	0.78	6.36
61 (oxidized)	*0.58*	*–1.83*	*0.90*	*0.02*	*0.288*	*–0.022*	*0.00*	*0.048*	*0.021*	*0.438*	*0.27*	*0.35*	*0.03*	*0.02*	*0.88*	*7.18*
67	1.88		0.91		0.310		0.67	0.157	0.022	0.140	0.27	0.34		0.08	0.83	6.80
67 (oxidized)	*0.75*	*–1.13*	*0.82*	*–0.09*	*0.252*	*–0.058*	*0.0034*	*0.063*	*0.018*	*0.286*	*0.23*	*0.30*	*–0.04*	*0.03*	*0.79*	*6.49*

[1] supposing an N/C atomic ratio of 0.02 in the organic matter
[2] estimated from N_{inorg} (the negative values are related probably to error of NH_4^+ estimation)
[3] estimated, supposing H/C=0.5 atomic ratio in the organic matter
[4] fixed most probably in OH^- and H_2O
[5] from H_{inorg}, subtracting the H fixed in ammonium

The C contents of the decarbonated samples varied between 1.00 and 2.41 weight %, while those of the decarbonated and oxidized samples varied between 0.56 and 0.75%. Since the color of the oxidized samples had changed from black and dark gray to very light gray and white, it was assumed that any remaining C was bonded to mixtures of relic (or included) carbonate minerals, salts of organic acids and relic or included, unoxidized organic matter. However, we offer no analytical proof for any of these assumptions at present.

The proportions of H in the organic and inorganic phases were estimated using literature data relating the decrease of the atomic H/C ratio with advancing maturation of dispersed organic matter (Durand, 1980; Tissot & Welte, 1984). The samples studied are in the organic maturity stage of metagenesis, where the elimination of hydrogen and heteroelements is advanced, yet rather slow. At such a stage, the carbon content of the dispersed organic matter is higher than 90 weight %, and the H/C atomic ratio varies between 0.2 and 0.5. The behavior of the nitrogen/carbon (N/C) atomic ratio during organic maturation is not fully understood. However, it is known that N/C atomic ratio will decrease with increasing organic maturation. The majority of nitrogen is lost along with aromatic hydrogen at the anthracite and metaanthracite stages (Boudoun & Espitalié, 1995; Sajgó, 1998), in which the samples of this study fall. Thus, the most probable N/C atomic ratio values would range from 0.005 to 0.02.

Let us suppose that the total C content values in Table 5 were bound to organic phases and the H/C and N/C atomic ratios in the organic matter were maximum values, *i.e.*, 0.5 and 0.02, respectively. Using these ratios, we calculated the H_{org} and N_{org} contents from the total (supposedly organic) C contents. Subtracting these H_{org} and N_{org} values from the total H and N values we obtained the H_{inorg} and N_{inorg} values. From the N_{inorg} values we could easily calculate the NH_4^+ contents bonded to inorganic phase(s). The remaining H_{inorg} was most probably present as OH^- and/or H_2O (Table 5). Considering that we have used the maximum H/C and N/C atomic ratios, and that all the C content was assumed to be organic, the H_{inorg} and N_{inorg} values and the calculated water and NH_4^+ contents are minimum estimates. The actual water and ammonium contents must have been somewhat higher.

The H_2O contents assessed in this way varied within a relatively small range between 5.6 and 7.2 weight %. Considering that dioctahedral white mica-like structures were predominant and chlorite was significant in the modal compositions of the <2 μm fraction samples (Table 3), the estimates were deemed reliable. Depending on the stage in reaction progress, the H_2O contents of illite-muscovite could range between *ca.* 4.5 and 10 weight %, while that of the chlorite could be between *ca.* 10 and 12 weight %.

The calculated NH_4^+ contents ranged between 0.19 and 0.35 weight %. The differences between the decarbonated and decarbonated and oxidized samples varied between -0.04 and 0.10 weight %. These differences are most probably related to the oxidation of organic matter, and, being one order of magnitude smaller than the concentrations themselves, suggest that the overwhelming majority of the NH_4^+ should be fixed by inorganic phase or phases. (The negative values can not be explained in this way; they may relate most probably to the error of NH_4^+ estimation.)

The highest NH_4^+ estimates were found in the Fläscherberg (Nos. 61 and 67) and the Brienz (No. 4) samples. The lowest NH_4^+ contents were determined in the Calfeisental (No. 41) sample containing evolved white mica with epizonal KI values and also in the Klausenpass samples (Nos. 36–39) showing variable KI values.

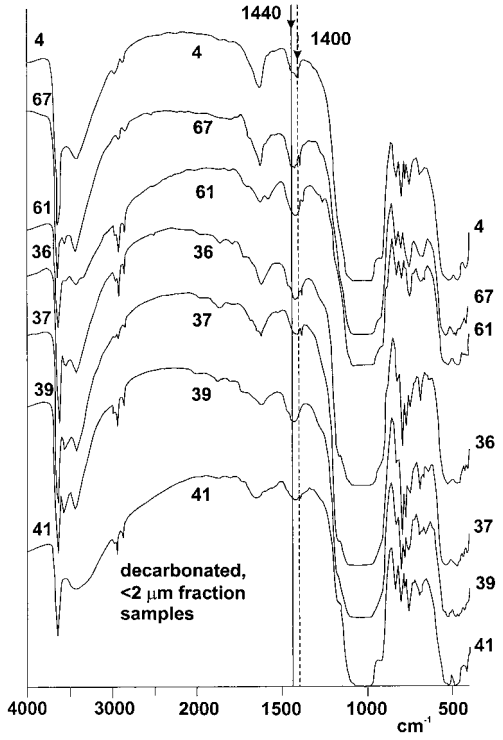

Fig. 8. FTIR spectra of decarbonated < 2 μm size fraction samples.

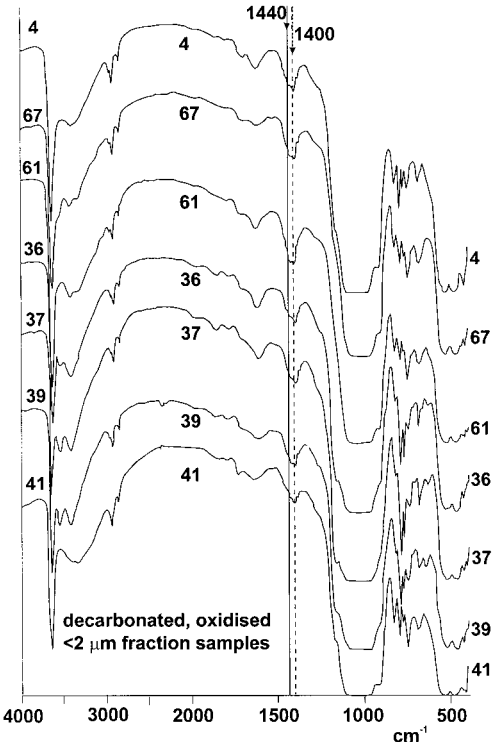

Fig. 9. FTIR spectra of decarbonated and oxidized, <2 μm size fraction samples.

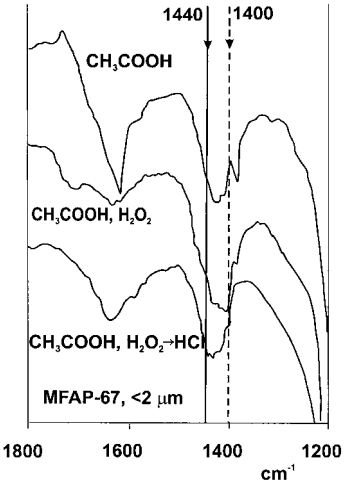

Fig. 10. Absorption bands of NH_4^+ measured in sample 67 pre-treated with acetic acid, hydrogen peroxide and subsequently, with hydrochloric acid. Note that there are no significant differences among the IR absorption intensities between 1400 and 1440 cm^{-1}.

IR signatures

Fig. 8 shows the IR absorption spectra of selected <2 μm fraction samples after de-carbonation with acetic acid. The spectra were very similar in the range of 400–1400 cm^{-1}. There were two very strong absorption bands between 400 and 600 cm^{-1} wavenumber. The band at 532 cm^{-1} could be attributed to the bending vibration of Si-O-Al bonds, and the band at 479 cm^{-1} was assigned to the bending vibration of Si-O-Si. There was a very strong absorption band at about 1040 cm^{-1} arising from the Si-O-Si stretching vibration. In the range of 600–1000 cm^{-1} there were several absorption bands with different intensities arising from Si-O stretching and Al-O-Si bending vibrations. The bending vibration of OH groups near to 1630 cm^{-1} appeared in every case. The difference in IR spectra of samples could be found in the higher wavenumber range between 3000 and 3700 cm^{-1}. In the IR spectra of sample No. 4 there was a strong but broad absorption band at 3403 cm^{-1} arising from the OH stretching vibration. Another strong and sharp absorption band was present at 3628 cm^{-1} due to the Al-OH stretching vibration. According to the XRPD analyses, illite-muscovite is the main mineral component of sample 4 (see also Table 3). In the IR spectra of some samples, another strong, sharp absorption band appears at 3555 cm^{-1} wavenumber arising from the Al-OH stretching vibration that could be attributed the presence of considerable amounts of chlorite.

Relatively broad and weak absorption bands appeared between 1400 and 1440 cm^{-1} wavenumbers with maxima between *ca.* 1410 and 1430 cm^{-1}. According to data from the literature, the band at 1400 cm^{-1} was due to the NH_4^+ deformational vibration in NH_4^+ salts (see, *e.g.*, Ryskin, 1974), whereas the band near to 1440 cm^{-1} is assigned to the NH_4^+ ion in the interlayer site of clay minerals (Šucha *et al.*, 1993; Petit *et al.*, 1998, 1999, *etc.*). (As a cautionary note: certain clay minerals, especially smectites, may undergo cation exchange between the KBr base pellets and NH_4^+-bearing minerals, *e.g.*, Petit *et al.*, 1998. This phenomenon may be – at least partly – responsible for the small variations in positions of band maxima, assuming an exchange of NH_4^+ by K^+ at relatively weakly bonded positions like crystal edges, terminations, *etc.*)

On the basis of IR spectra, the highest concentrations of NH_4^+ were found in samples 67, 61 and 4, while the lowest concentration was in sample 41. This is in agreement with the conclusions deduced from the estimates based on elemental analyses (Table 5).

Similar conclusions could be drawn from the IR spectra of the decarbonated and oxidized samples (Fig. 9). Most of the maximum positions of the NH_4^+ absorption band were shifted to 1402–1404 cm^{-1}, but had shoulders at around 1430 cm^{-1} wavenumber.

Greater details of the IR spectra between 1800 and 1200 cm^{-1} are given in Fig. 10. In case of sample 67, repeated decarbonation by HCl was applied in an attempt to dissolve all traces of carbonate minerals that would affect the absorption spectra. However, the intensity of the absorption band was not decreased significantly after these treatments. This suggested that the band at *ca.* 1430 cm^{-1} wavenumber may be attributed to NH_4^+ fixed in the interlayer site of a phyllosilicate. The most probable candidate for the host of NH_4^+ is the abundant dioctahedral white mica (see also Table 3).

STEM, AEM and EELS results

The data presented earlier has shown indirectly that NH_4^+ was indeed present and most likely in the white mica interlayer site. STEM EDS and EELS analyses were performed to directly observe the presence of NH_4^+ and to determine the spatial distribution of the interlayer cations. EDS analyses were relatively insensitive to N, but they could collect information about the other interlayer cations such as Na, K and Ca.

The STEM EDS images presented in Fig. 11 showed that K was the dominant interlayer cation in the white mica of sample 67 (Fläscherberg locality), while Na was also present in lesser amounts. In the images of K and Na, there are some features that need further explanation. The feature running north-to-south in all the images corresponds to a parting of one half of the mica sheet that does not extend all the way through the crystal. This gives a reduction in intensity in the K and Na X-ray maps and can be clearly seen in the bright-field (BF) image (labeled Cleavage). Other regions show increased intensity in the K, Na and O maps due to overlapping crystals (labeled Overlap). The Ca and S images are identical, showing that Ca is related to Ca-sulfate contamination and not to the margarite content of the white mica. (K,Na)Cl is also present, which probably formed as a daughter crystal of a fluid inclusion (labeled Salt). One feature which does not correspond to anything visible in the BF STEM or CTEM image is the linear contrast that shows a decrease in K and a corresponding increase in Na (labeled by arrows). These features seem to be a crystallographically controlled segregation of K and Na within the basal plane of the mica. The linear variations in K and Na are very similar to those described by Livi & Veblen (2002) in the mixed Na-K micas from the Liassic black shales of the Glarus Alps, Switzerland. In those samples, the segregation of Na, Ca, and K formed nanometer-scale domain structures within the basal layers. However, the concentration of Ca, Na was higher in the Liassic samples than in our study. Regardless

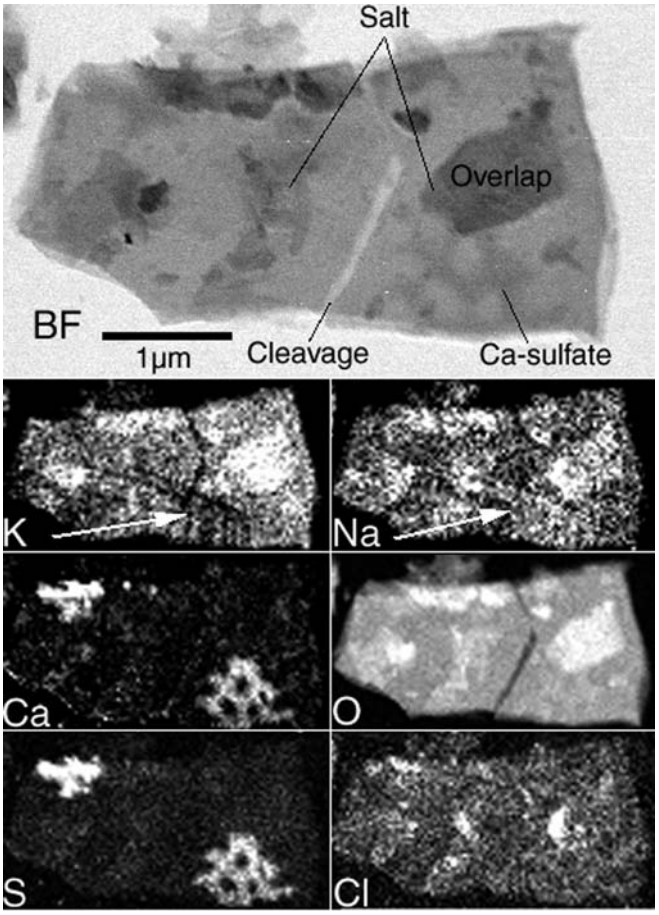

Fig. 11. Variations of chemical compositions within a metamorphic (authigenic) dioctahedral white mica flake from sample MFAP-67, as determined by STEM EDS. See text for explanation of labels.

of their total concentration, the X-ray images suggest that similar disequilibrium domain-like intergrowths are present within the basal plane of sample 67. This is in contrast to the more typical concept of regular or irregular interstratification of muscovite and paragonite layers.

Electron energy loss spectroscopy was used to detect the presence of nitrogen within the white micas. Similar investigations were made in Nieto *et al.* (2001) where N *K* EELS absorption edges were detected in tobelitic micas. The small N peak present in Fig. 12a was derived from a single crystal of white mica and is direct evidence that nitrogen is in the mica interlayer site. The Ca $L_{2,3}$ peak comes from Ca-sulfate contamination found in the X-ray maps. This small amount of N was compared to the N found in the tobelitic sample in Fig. 12b. The atomic ratio of N/K could be estimated by the method of Egerton (1996). The N/K for the tobelitic sample was 1.9 whereas sample 67 yielded a ratio of 0.01.

Conclusions

In the present paper, dioctahedral white micas with "anomalous" illite Kübler indices have been reported from marly and silty shale and slate lithologies found in different locali-

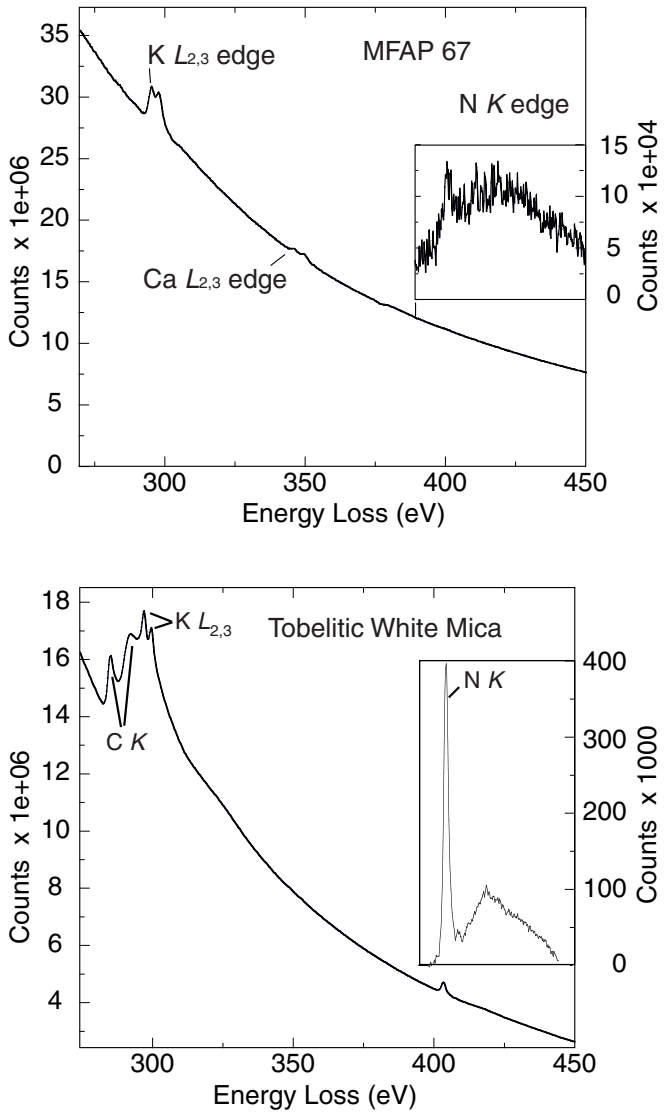

Fig. 12. a) Details of EEL (electron energy loss) spectrum of a metamorphic white mica flake from sample MFAP-67, showing the signatures of K and the presence of N (see the inset). Ca comes from Ca-sulfate contamination. b) EEL spectrum of a tobelitic white mica from Nieto *et al.* (2001) and Nieto (2002). Carbon comes from the support film.

ties of the Helvetic zone, Swiss Central Alps. The Kübler index values showed systematically lower apparent metamorphic grades than the regional patterns constructed and published by Frey *et al.* (1999), and are in conflict with the new chlorite "crystallinity" and vitrinite reflectance data presented here.

Detailed XRPD studies showed that this "anomalous" 10 Å phase was a K-dominant dioctahedral white mica structure (called illite-muscovite) with minor amounts of swelling (smectitic) interstratifications. In addition, a metastable mixed K>>Na>NH_4^+ mica with a domain-like structure was found and was often associated with traces of a discrete paragonite phase.

Based on the organic maturity conditions, the C, H and N elemental compositions of the decarbonated and oxidized <2 μm fraction, and the XRPD patterns, inorganic N may be present in form of NH_4^+. The amount of NH_4^+ varied between *ca.* 0.2 and 0.4 weight %. Infrared absorption spectra of these clay-size fractions unequivocally proved the presence of NH_4^+ – the overwhelming majority of which was fixed in inorganic phase(s).

STEM and EDS observations, complemented by EELS determinations, suggested that the nitrogen was fixed in the dioctahedral white mica structures. These white micas were characterized as containing domain-like variations of K and Na (and probably NH_4^+) with K being always dominant. Thus, a metastable dioctahedral white mica with mixed (K>>Na> NH_4^+) interlayer occupancy seems to be a reliable model for the 10 Å phase in question. This model agreed fairly well with those elaborated for the K-Na-Ca mixed micas by Livi *et al.* (1997), Livi & Veblen (2002), and for the mixed K-NH_4^+ micas by Nieto (2002).

These samples represent metastable disequlibrium products of the phyllosilicate reaction progress during very low-grade metamorphism. Judging from their occurrences in the Helvetic zone of the Swiss Central Alps and in many other parts of the world, these mineral structures may be much more widespread than it has been anticipated so far, and they may lead to erroneous determination of metamorphic grade when illite Kübler index ("crystallinity") method is used routinely.

Acknowledgements: The field works for collecting the samples from the Swiss Alps formed a part of the projects Nos. 20-50'652.97 and 20-50'6842.99 "Studies in Very Low-Grade Metamorphism" headed by M.F. and supported by the Schweizerischer Nationalfonds zur Förderung der Wissenschaftlichen Forschung. Great part of the laboratory work (XRPD, vitrinite reflectance, *etc.*) was financially supported by the Hungarian Research Fund (OTKA), Budapest, program No. T-035050/2001-2004 to P.Á. The authors thank the technical co-workers of the Laboratory for Geochemical Research, Hungarian Academy of Sciences, Budapest for their assistance. Thus, thanks are due to Mrs. O. Komoróczy, Cs.M. Sándor, Ms. K. Temesvári and N. Keresztes for XRD analyses, to Mrs. P. Maróth for work with IR and to Ms. N. Szász for preparing polished thin sections. Thanks are due to Dr. Dennis D. Eberl and Dr. Raffaele Sassi for thoroughly reviewing and improving the manuscript.

References

Árkai, P. (1983): Very low- and low-grade Alpine regional metamorphism of the Paleozoic and Mesozoic formations of the Bükkium, NE-Hungary. *Acta Geol. Hung.*, **26**, 83-101.

– (2002): Phyllosilicates in very low-grade metamorphism: Transformation to micas. *in* "Micas: Crystal Chemistry and Metamorphic Petrology", Reviews in Mineralogy and Geochemistry, Vol. **46**, A. Mottana, F.P. Sassi, J.B. Thompson, S. Guggenheim, eds. Mineralogical Society of America, Blacksburg, Virginia, 463-478.

Árkai, P., Sassi, F.P., Sassi, R. (1995): Simultaneous measurements of chlorite and illite crystallinity: a more reliable geothermometric tool for monitoring low- to very low-grade metamorphism in metapelites. A case study from Southern Alps (NE. Italy*). Eur. J. Mineral.*, **7**, 1115-1128.

Árkai, P., Fenninger, A., Nagy, G. (2002): Effects of lithology and bulk chemistry on phyllosilicate reaction progress in the low-T metamorphic Graz Paleozoic, Eastern Alps, Austria. *Eur. J. Mineral*., **14**, 673-686.

Bárdossy, Gy. (1966): A bauxit ásványos összetételének röntgendiffrakciós vizsgálata. (Investigation of modal composition of bauxite by X-ray diffractometry.) *Kohászati Lapok*, **99**, 335-363. (In Hungarian).

Bárdossy, Gy., Bottyán, L., Gadó, P., Griger, Á, Sasvári, J. (1980): Automated quantitative phase analysis of bauxites. *Am. Mineral.*, **65**, 135-141.

Bárdossy, Gy., Árkai, P., Fodor, J. (2001): Application of the fuzzy set theory to the quantitative analysis of rocks by X-ray diffractometry. *Földtani Közlöny*, **131**, 331-341. (In Hungarian, with an extended English abstract.)

Barrer, R.M. & Denny, P.J. (1961): Hydrothermal chemistry of the silicates. Part IX. Nitrogeneous aluminosilicates. *J. Chem. Soc.,* Part **1**, 971-1000.

Barrer, R.M. & Dicks, L.W.R. (1966): Chemistry of soil minerals. Part III. Synthetic micas with substitutions of NH_4 for K, Ga for Al and Ge for Si. *J. Chem. Soc*., **A**, 1379-1385.

Bobos, I. & Ghergari, L. (1999): Conversion of smectite to ammonium illite in the hydrothermal system of Harghita Băi, Romania: SEM and TEM investigations. *Geologica Carpathica*, **50**, 379–387.

Boudou, J.P. & Espitalié, J. (1995): Molecular nitrogen from coal pyrolysis: Kinetic modelling. *Chemical Geol.*, **126**, 319-333.

Compton, J.S., Williams, L.B., Ferrell, Jr. R.E. (1992): Mineralization of organogenic ammonium in the Monterey Formation, Santa Maria and San Joaquin basins, California, USA. *Geochim. Cosmochim. Acta*, **56**, 1979-1991.

Cooper, J.A. & Abedin, K.Z. (1981): The relationship between fixed ammonium-nitrogen and potassium in clays from a deep well on the Texas Gulf Coast. *Texas J. Sci*., **33**, 103-111.

Daniels, E.J. & Altaner S.P. (1990): Clay mineral authigenesis in coal and shale from the Anthracite region, Pennsylvania. *Am. Mineral.*, **75**, 825-839.

Drits, V.A., Lindgreen, H., Salyn, A.L. (1997): Determination of the content and distribution of fixed ammonium in illite-smectite by X-ray diffraction: Application to North Sea illite-smectite. *Am. Mineral.*, **82**, 79-87.

Drits, V.A., Lindgreen, H., Sakharov, B.A., Jakobsen, H.J., Salyn, A.L., Dainyak, L.G. (2002): Tobelitization of smectite during oil generation in oil-source shales. Application to North Sea illite-tobelite-smectite-vermiculite. *Clays and Clay Minerals*, **50**, 83-98.

Duit, W., Jansen, J., Ben, H., Van Breemen, A., Bos, A. (1986): Ammonium micas in metamorphic rocks as exemplified by Dôme de l'Agout (France). *Am. J. Sci.*, **286**, 702-732.

Durand, B. (1980): Kerogen. Insoluble organic matter from sedimentary rocks. Edition Technip, Paris.

Egerton, R.F. (1996): Electron energy-loss spectroscopy in the electron microscope, Second edition. Plenum, New York, 485 pp.

Eugster, H.P. & Munoz, J. (1966): Ammonium micas: Possible sources of atmospheric ammonia and nitrogen. *Science*, **151**, 683-686.

Farmer, V.C. (ed.) (1974): Infrared Spectra of Minerals. Mineralogical Society, London.

Frey, M. (1969): A mixed-layer paragonite/phengite of low-grade metamorphic origin. *Contrib. Mineral. Petrol*., **14**, 63-65.

– (1987): Very low-grade metamorphism of clastic sedimentary rocks. *in* "Low Temperature Metamorphism", M. Frey, ed. Blackie, Glasgow, 9-58.

Frey, M. & Niggli, E. (1972): Margarite, an important rock-forming mineral in regionally metamorphosed low-grade rocks. *Die Naturwissenschaften*, **59**, 214-215.

Frey, M., Desmons, J., Neubauer, F. (eds.) (1999): Metamorphic maps of the Alps, 1:500.000. *Enclosure of the Schweizerische Mineralogische und Petrographische Mitteilungen*, **79**, 1.

Guidotti, C.V. & Sassi, F.P. (1998): Petrogenetic significance of Na-K white mica mineralogy: Recent advances for metamorphic rocks. *Eur. J. Mineral.*, **10**, 815-854.

Hallam, M. & Eugster, H.P. (1976): Ammonium silicate stability relations. *Contrib. Mineral. Petrol.*, **57**, 227-244.

Higashi, S. (1978): Dioctahedral mica minerals with ammonium ions. *Mineral. J.*, **9**, 16-27.

Higashi, S. (1982): Tobelite, a new ammonium dioctahedral mica. *Mineral. J.*, **11**, 138-146.

Juster, T.C., Brown, P.E., Bailey, S.W. (1987): NH_4-bearing illite in very low grade metamorphic rocks associated with coal, northeastern Pennsylvania. *Am. Mineral.*, **72**, 555-565.

Kisch, H.J. (1983): Mineralogy and petrology of burial diagenesis (burial metamorphism) and incipient metamorphism in clastic rocks. *in* "Diagenesis of Sediments and Sedimentary Rocks, 2" G. Larsen & G.V. Chilingar, eds., Elsevier, Amsterdam, 289-493.

Kozáč, J., Očenáš, D., Derco, J. (1977): Amónna hydrosl'uda vo Vihorlate. The discovery of ammonium hydromica in the Vihorlat Mts. (Eastern Slovakia). *Mineralia slovaca, Bratislava*, **9**, 479–494.

Kübler, B. (1967): La cristallinité de l'illite et les zones tout a fait superieures du métamorphisme. *in* "Étages tectoniques, Colloque de Neuchâtel 1966", A La Baconniere, Neuchâtel, 105-121.

– (1990): "Cristallinité" de l'illite et mixed-layers: breve révision. *Schweiz. Mineral. Petrogr. Mitt*., **70**, 89-93,

Langford, J.I. (1978): A rapid method for analyzing the breadth of diffraction and spectral lines using the Voigt function. *J. Appl. Cryst.*, **11**, 10-14.

Levinson, A.A. & Day, J.J. (1968): Low temperature hydrothermal synthesis of montmorillonite, ammonium-micas and ammonium-zeolites. *Earth Planet. Sci. Lett.*, **5**, 52-54.

Lindgreen, H., Drits, V.A., Sakharov, B.A., Salyn, A.L., Wrang, P., Dainyak, L.G. (2000): Illite-smectite structural changes during metamorphism in black Cambrian Alum shales from the Baltic area. *Am. Mineral.*, **85**, 1223-1238.

Liu, Q., Zhang, P., Ding, S., Lin, X., Zheng, N. (1996): NH_4-illite in Permocarboniferous coal-bearing strata, North China. *Chinese Sci. Bull*., **41**, 1458-1461.

Livi, K.J.T. & Veblen, D.R. (2002): White micas of mixed composition: Does mixed-layered Pa-Mu exists? International Mineralogical Association meeting in Edinburgh, Scotland.

Livi, K.J.T., Veblen, D.R., Ferry, J.M., Frey, M. (1997): Evolution of 2:1 layered silicates in low-grade metamorphosed Liassic shales of Central Switzerland. *J. metamorphic Geol*., **15**, 323-344.

Livi, K.J.T., Abad, I., Veblen, D., Nieto, F. (2001): EELS analysis of Micas. *J. Conference Abstracts, 2001, EUG XI, Strasbourg,* 673.

Livi, K.J.T., Ferry, J.M., Veblen, D.R., Frey, M., Connolly, J.A.D. (2002): Reactions and physical conditions during metamorphism of Liassic aluminous black shales and marls in central Switzerland. *Eur. J. Mineral*., **14**, 647-672.

van der Marel, H. W. & Beutelspacher, H. (1976): Atlas of Infrared Spectroscopy of Clay Minerals and their Admixtures. Elsevier Amsterdam, Oxford, New York.

Merriman, R.J. & Frey, M. (1999): Patterns of very low-grade metamorphism in metapelitic rocks. 61-107.

Merriman, R.J. & Peacor, D.R. (1999): Very low-grade metapelites: mineralogy, microfabrics and measuring reaction progress. *in*

"Low-Grade Metamorphism", M. Frey & D. Robinson, eds. Blackwell Science, Oxford, 10-60.

Nieto, F. (2002): Characterization of coexisting NH_4- and K-micas in very low-grade metapelites. *Am. Mineral.*, **87**, 205-216.

Nieto, F., Abad, I., Livi, K.J.T., (2001): Tobelite in low-grade metamorphic organic-rich shales from Douro-Beira, Portugal. *J. Conference Abstracts,* **2001***, EUG 11,* 231.

Petit, S., Righi, D., Madejová, J., Decarreau, A. (1998): Layer charge estimation of smectites using infrared spectroscopy. *Clay Minerals*, **33**, 579-591.

–, –, – (1999): Interpretation of the infrared NH_4^+ spectrum of the NH_4^+-clays: application to the evolution of the layer charge. *Clay Minerals*, **34**, 543-549.

Ryskin, Y.I. (1974): The vibration of protons in minerals: hydroxyl, water and ammonium. *in* "The Infrared Spectra of Minerals", V. C. Farmer, ed. Monograph No. 4, Mineralogical Society, London, 137-181.

Sajgó, Cs. (1998): On-line pyrolysis-gas chromatographic studies on organic matter of sedimentary rocks (Manuscript in Hungarian). 1-117.

Sakharov, B.A., Lindgreen, H., Salyn, A., Drits, V.A. (1999): Determination of illite-smectite structures using multispecimen X-ray diffraction profile fitting. *Clays and Clay Minerals*, **47**, 555-566.

Schroeder, P.A. & McLain, A.A. (1998): Illite-smectites and the influence of burial diagenesis on the geochemical cycling of nitrogen. *Clay Minerals*, **33**, 539-546.

Shigorova, T.A., Kotov, N.V., Kotel'nikova, Ye.N., Shamakin, B.M., Frank-Kamenetskiy, V.A. (1981): Synthesis, diffractometry, and IR spectroscopy of micas in the series from muscovite to the ammonium analog. *Geochemistry International*, **18**, 76-82.

Sterne, E.J., Reynolds Jr., R.C., Zantop, H. (1982): Natural ammonium illites from black shales hosting a stratiform base metal deposit, DeLong Mountains, Northern Alaska. *Clays and Clay Minerals*, **30**, 161-166.

Stevenson, F.J. & Dhariwal, A.P.S. (1959): Distribution of fixed ammonium in soil. *Soil Science Society of America Proceedings*, **23**, 121-125.

Šucha, V. & Širáňová, V. (1991): Ammonium and potassium fixation in smectite by wetting and drying. *Clays and Clay Minerals*, **39**, 556–559.

Šucha, V., Konečný, V., Lexa, J., Gerthofferová, H. (1993): Syngenetic alteration of andesite volcanoclastic rocks of the Neresnica Formation in an aquatic environment (Javorie, Western Carpathians). *Geologica Carpathica – Series Clays, Bratislava*, **44**, 43–48.

Šucha, V., Kraus, I., Madejová, J. (1994): Ammonium illite from anchimetamorphic shales associated with anthracite in the Zemplenicum of the Western Carpathians. *Clay Minerals*, **29**, 369-377.

Šucha, V., Elsass, F., Eberl, D.D., Kuchta, L., Madejová, J., Gates, W.P., Komadel, P. (1998): Hydrothermal synthesis of ammonium illite. *Am. Mineral.*, **83**, 58-67.

Teichmüller, M. (1987): Organic material and very low-grade metamorphism. *in* "Low Temperature Metamorphism", M. Frey, ed. Blackie, Glasgow, 114-161.

Tissot, B. & Welte, D.H. (1984): Petroleum Formation and Occurrence. Springer, Berlin.

Tsunashima, A., Kanamaru, F., Ueda, S., Koizumi, M., Matsushita, T. (1975): Hydrothermal syntheses of amino acid montmorillonites and ammonium-micas. *Clays and Clay Minerals*, **23**, 115-118.

Vedder, W. (1965): Ammonium in muscovite. *Geochim. Cosmochim. Acta*, **29**, 221-228.

Voncken, J.H.L., Wevers, J.M.A.R., van der Erden, A.J.M., Bos, A., Jansen, J.B.H. (1987): Hydrothermal synthesis of tobelite, $NH_4Al_2Si_3AlO_{10}(OH)_2$, from various starting material and implications for its occurrence in nature. *Geol. Mijnb.*, **66**, 259-269.

Ward, C.R. & Christie, P.J. (1994): Clays and other minerals in coal seams of the Moura-Baralaba area, Bowen Basin, Australia. *Int. J. Coal Geol.*, **25**, 287-309.

Williams, L.B. & Ferrell Jr., R.E. (1991): Ammonium substitution in illite during maturation of organic matter. *Clays and Clay Minerals*, **39**, 400-408.

Williams, L.B., Ferrell Jr., R.E., Chinn, E.W., Sassen, R. (1989): Fixed-ammonium in clays associated with crude oils. *Applied Geochemistry*, **4**, 605-616.

Wilson, P.N., Parry, W.T., Nash, W.P. (1992): Characterization of hydrothermal tobelitic veins from black shale, Oquirrh Mountains, Utah. *Clays and Clay Minerals*, **40**, 405-420.

Wright, A.C., Granquist, W.T., Kennedy, J.V. (1972): Catalysis by layer lattice silicates. I. The structure and thermal modification of a synthetic ammonium dioctahedral clay. *J. Catalysis*, **25**, 65-80.

Yamamoto, T. (1967): Mineralogic studies of sericites associated with Roseki ores in the western part of Japan. *Mineral. J.*, **5**, 77-97.

Yamamoto, T. & Nakahira, M. (1966): Ammonium ions in sericites. *Am. Mineral.*, **51**, 1775-1778.

Received 9 May 2003
Modified version received 18 December 2003
Accepted 11 February 2004